Int. J. Heat Mass Transfer. Vol. 36, No. 6, pp. 1445–1457, 1993
Printed in Great Britain

0017-9310/93 $6.00 + 0.00

An extension of the fire-field modelling technique to include fire–sprinkler interaction—II. The simulations

N. A. HOFFMANN and E. R. GALEA
Centre for Numerical Modelling and Process Analysis, The University of Greenwich, London, U.K.

(*Received* 17 *September* 1991 *and in final form* 28 *August* 1992)

Abstract—The Eulerian–Eulerian fire–sprinkler model outlined in a companion paper is applied to simulate two distinct fire–sprinkler scenarios. The predicted results and comparisons with experimental data are presented. These indicate good agreement near the sprinkler source, which deteriorates in the far field. The considerable increase in the amount of computational effort involved in these calculations is also highlighted, pointing towards the utilization of parallel computing techniques.

1. INTRODUCTION

IN A COMPANION paper [1] the authors described the basis of a mathematical model for simulating the effects of a sprinkler activated within a fire compartment. In this paper the model is applied to two fire–sprinkler scenarios for which experimental data are available in an attempt to demonstrate the applicability of the models.

Mathematical field modelling of fires and smoke spread in enclosures has been underway for a number of years [2]. At its heart lies the numerical solution of the Navier–Stokes equations. The considerably more complicated problem of fire–sprinkler interaction also lends itself to this form of analysis. There are now two physical phases, the gas phase involving the general fluid circulation of the hot combustion products and the liquid phase, representing the evaporating water droplets. Using the Eulerian–Eulerian approach the second phase is treated as a continua with its own set of conservation equations. These two sets of equations are linked by a space-sharing equation and a set of auxiliary equations which describe the interphase processes of heat, mass and momentum transfer. This set of equations is solved numerically using the procedures SIMPLEST and IPSA as implemented in the computer program PHOENICS [3]. Details of the model and its implementation may be found in the companion paper [1].

2. FIRE–SPRINKLER SIMULATIONS IN PRACTICE

One of the difficulties in validating field fire models is the considerable quantity of detailed information predicted and the very difficult task of obtaining experimental data for comparison purposes.

Fortunately, experimental results were obtained for two distinct fire and sprinkler experiments. Comparisons between experimental fire–sprinkler data and model results are presented below.

Two fire–sprinkler scenarios have been investigated. These simulations concerned a corner fire located in an *open* office-sized compartment [4, 5] and a bed fire within a large *closed* hospital ward [6, 7].

The first experiment was carried out by the National Bureau of Standards [8] within an office sized compartment containing a wastepaper basket fire. The sprinkler was positioned remote from the fire source. The effect of a sprinkler nearly above the fire source was investigated in the second experiment. The data used was obtained by the Fire Research Station [9] during a series of eight fire tests within a hospital room. The experiments were carried out to discover whether a sprinkler could control a typical bed fire early enough to prevent life-hazardous conditions from occurring.

One of the benefits of fire modelling is the determination of temperature rise and general conditions within a compartment. Hence, subsequent impact on life can be investigated. One criteria for determining life threatening conditions is the level of the gas temperature, whereby it is recommended that the temperature should not exceed 50°C below 1.5 m from the floor [9]. The development and spread of this hot layer is of interest to evacuation and life safety studies and can be monitored during transient simulations.

2.1. *Office scenario*

The fire compartment, depicted in Fig. 1, represents an office of dimensions 2.44 m by 3.66 m in plan and 2.44 m in height. A doorway of dimensions 0.76 m in width and 2.03 m in height was situated on the far end of the room and was open throughout the scenario. The solution domain was extended to include the outside region in the immediate proximity to the door plane. This is necessary in order to obtain the correct pressure distribution and flow pattern

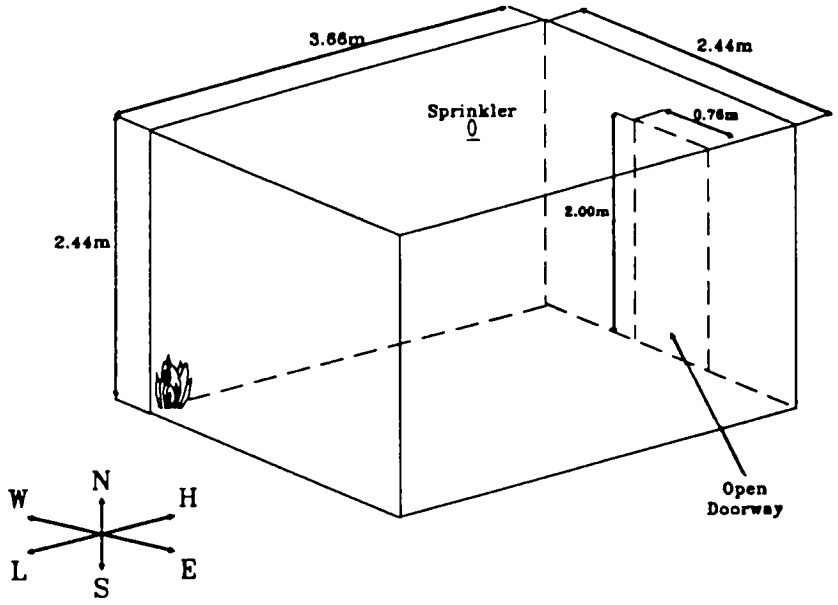

FIG. 1. Office schematic.

through the doorway [4, 10]. This room was fitted with a $12 \times 11 \times 20$ Cartesian grid, comprising of 1848 internal and 792 external cells. At the walls an isothermal condition with an ambient temperature of 24°C was assumed.

The office fire scenario itself took the form of a wastepaper basket fire initiation, whereby the office furniture which included a desk, chair and bookcase were all heavily loaded with a paper/book type fuel load. However, as precise information relating to the fire spread was not available the fire was represented as a volumetric heat source concentrated in a volume equal to the wastepaper basket of dimensions 0.3 m × 0.3 m × 0.3 m, situated within a corner opposite the doorway. The heat source had a time varying heat release rate as depicted in Fig. 2. The maximum power output is approximately 50 kW as suggested by the experimental data. The single phase simulation lasted for 175 s and was used as the initial state for the two-phase fire–sprinkler study. During the second stage, which lasted for 25 s, the fire was assumed to be still in progress. However, it was assumed that the heat output of the fire was reduced to a lower constant rate of 30 kW.

The effect of a single centrally positioned sprinkler was simulated. It was located 1.8 m from the fire and

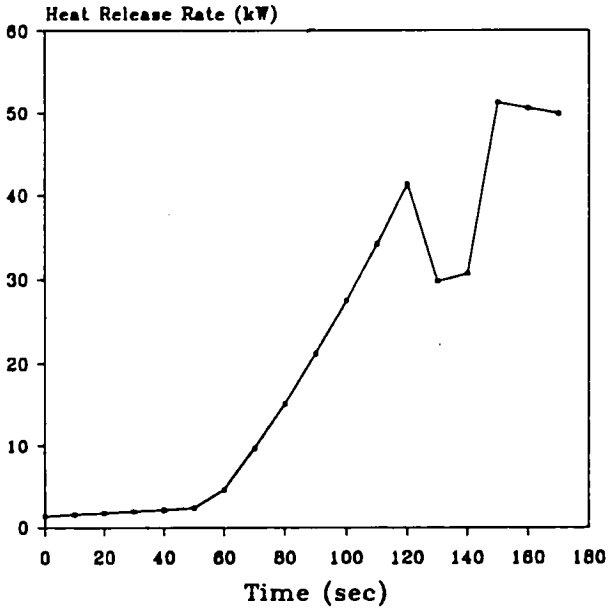

FIG. 2. Simulated office fire heat release rates.

0.1 m below the ceiling. The water was released at a rate of 0.596×10^{-3} m^3 s^{-1} at an angle of 70° from the sprinkler head line of symmetry. It was assumed that droplets with a uniform average diameter of 1 mm were released with an initial temperature of 10°C.

During the experiment temperature measurements were taken at two distinct locations within the room; near the centre and halfway between the sprinkler and the doorway. At these locations simulated sprinkler links with a Response Time Index (RTI) of 46 (ms)$^{1/2}$ were situated. These were instrumented with thermocouples to measure their temperature variation with height just below the ceiling. From these locations and the arrangement of the numerical grid used, two coinciding positions were chosen for comparison purposes. The first location just above the sprinkler is 0.05 m below the ceiling, whist the other near the doorway is 0.24 m below the ceiling.

In order to be able to compare the measured link temperatures with the model, the calculated gas temperatures were converted using the following temperature-response equation of the link [11]:

$$\frac{\mathrm{d}}{\mathrm{d}t}(\Delta T_c) = \frac{u^{1/2}}{\mathrm{RTI}}(\Delta T_g - \Delta T_c)$$

where u is the gas velocity, T_c the temperature of the sprinkler element and T_g the gas temperature.

2.2. *Hospital ward scenario*

The fire compartment, depicted in Fig. 3, was a six bed hospital room of dimensions 7.325 m by 7.85 m by 2.7 m. The flow domain was fitted with a $14 \times 15 \times 11$ Cartesian grid comprising of 2310 control volumes. The thermal conductivity and thickness of the walls, floor and ceiling were supplied and included in the calculations. In addition, six 1 kW oil-filled radiators situated on a wall were modelled using a single 6 kW heat source 7.85 m long, 0.3 m in width and 0.5 m high.

The method used to account for the heat losses through the walls was that used within the Harvard Zone Model [12]. It is based on the assumption that the heat transfer coefficient varies linearly with temperature between T_a and $(T_a + 100.0)$, where T_a is the ambient temperature, with fixed values outside this range. The boundary thermal resistance is then calculated from this and the conductive properties of the boundaries.

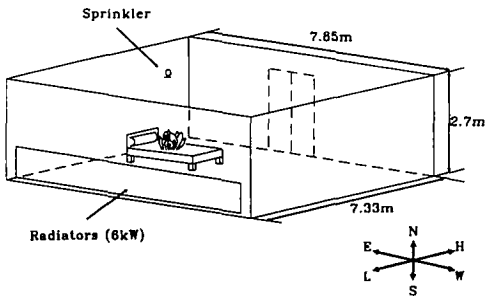

FIG. 3. Hospital room schematic.

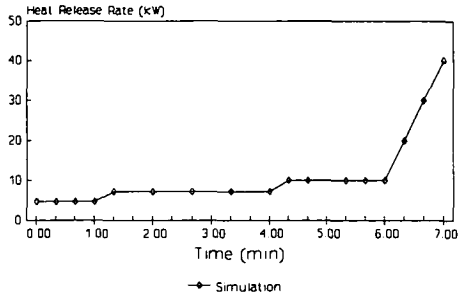

FIG. 4. Simulated hospital ward fire heat release rates.

In the experiment the fire was situated on a bed which was 1.35 m wide, 1.75 m in length and stood 0.5 m above the floor. The bed-head was positioned at the centre of the east wall. The sprinkler was located 0.353 m below the ceiling and 0.895 m from the east wall along the centre line of the room. Its characteristics were identical to those used in the office fire scenario.

As in the previous case, room conditions prior to the sprinkler activation were obtained by modelling only the fire. The results from the single-phase simulation, which lasted for 420 s, were used as initial values for the two-phase fire–sprinkler study. During the single-phase simulation the fire was ramped from 0 to 40 kW according to experimental data, see Fig. 4. The fire was modelled as a heat source occupying a fixed area of 0.45 m × 0.5 m, positioned 0.25 m from the east wall. After 420 s the sprinkler was activated. During this stage, which lasted for 120 s, the fire was maintained at a constant 40 kW; the heat release rate the fire possessed at the time of sprinkler activation.

During the test, gas temperatures were monitored at various heights and locations throughout the room. Two locations, 75 mm below the ceiling are shown below.

Both simulations were performed with a 1 s time step. During these steps iterations across the domain were carried out until convergence criteria of the variables solved for were satisfied; typically residuals around 1.0 E-4.

3. RESULTS

3.1. *Office scenario*

Comparisons between predicted and experimental sprinkler link temperatures before and after sprinkler activation are depicted in Fig. 5. Experimental monitoring sites were restricted to two locations.

The first, depicted in Fig. 5(a), is 0.05 m below the ceiling in the centre of the room. Figure 5(b) illustrates the effect more remote from the sprinkler at a position near the doorway, 0.24 m below the ceiling. These suggest that the correct trends in temperature variation have been captured. Experimental and numerical uncertainties concerned with the fire load and the

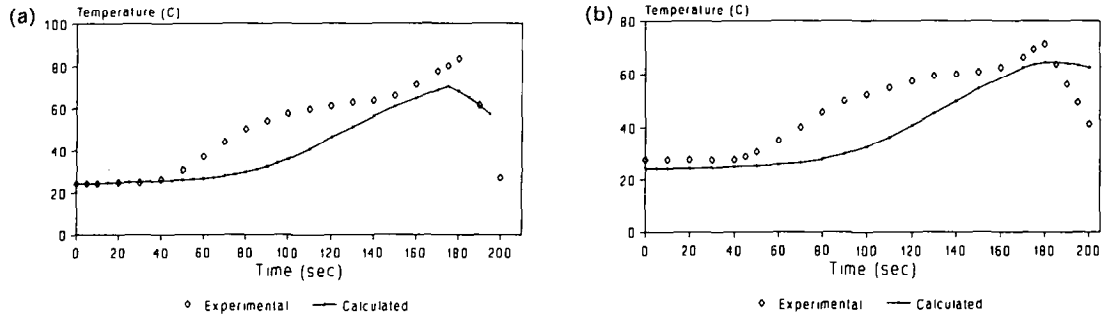

FIG. 5. Office fire: predicted and measured sprinkler link temperatures. (a) Towards the centre of the room, 0.05 m below the ceiling. (b) Near the door, 0.24 m below the ceiling.

coarseness of the numerical grid contribute towards the observed discrepancies.

The effect the sprinkler has on the office environment is illustrated in Figs. 6 and 7. These diagrams depict gas temperatures and velocity vectors before and 25 s after sprinkler activation. No experimental data are available to verify these results.

Figure 6 depicts gas temperatures on a vertical plane along the length of the room passing through the sprinkler and the centre line of the doorway. They show how the stable temperature stratification within the room is disturbed by the injected water spray. The cooling effect the water spray has on the gases is illustrated by the reduced gas temperature which exists

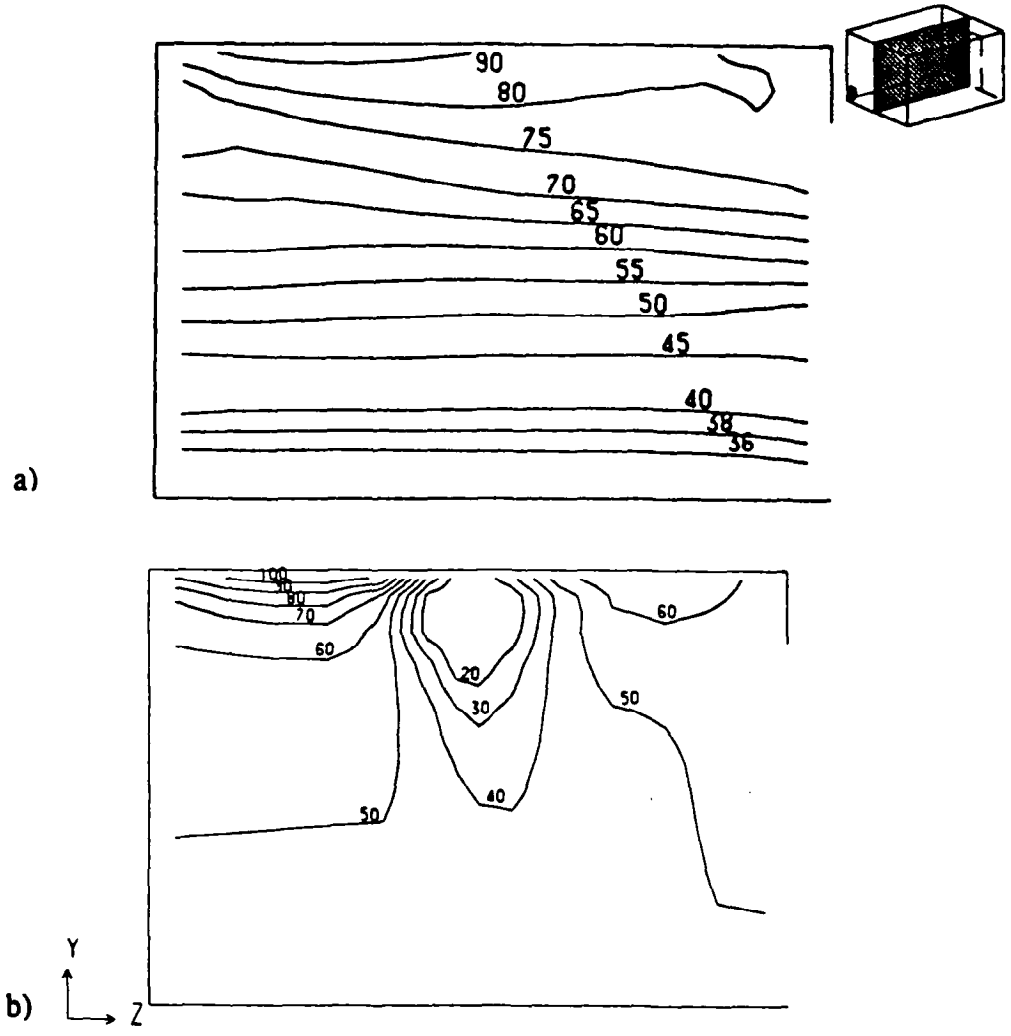

FIG. 6. Side view of office: predicted gas temperature contours on the vertical plane through the sprinkler and doorway. (a) Fire only (175 s). (b) Fire and sprinkler (200 s).

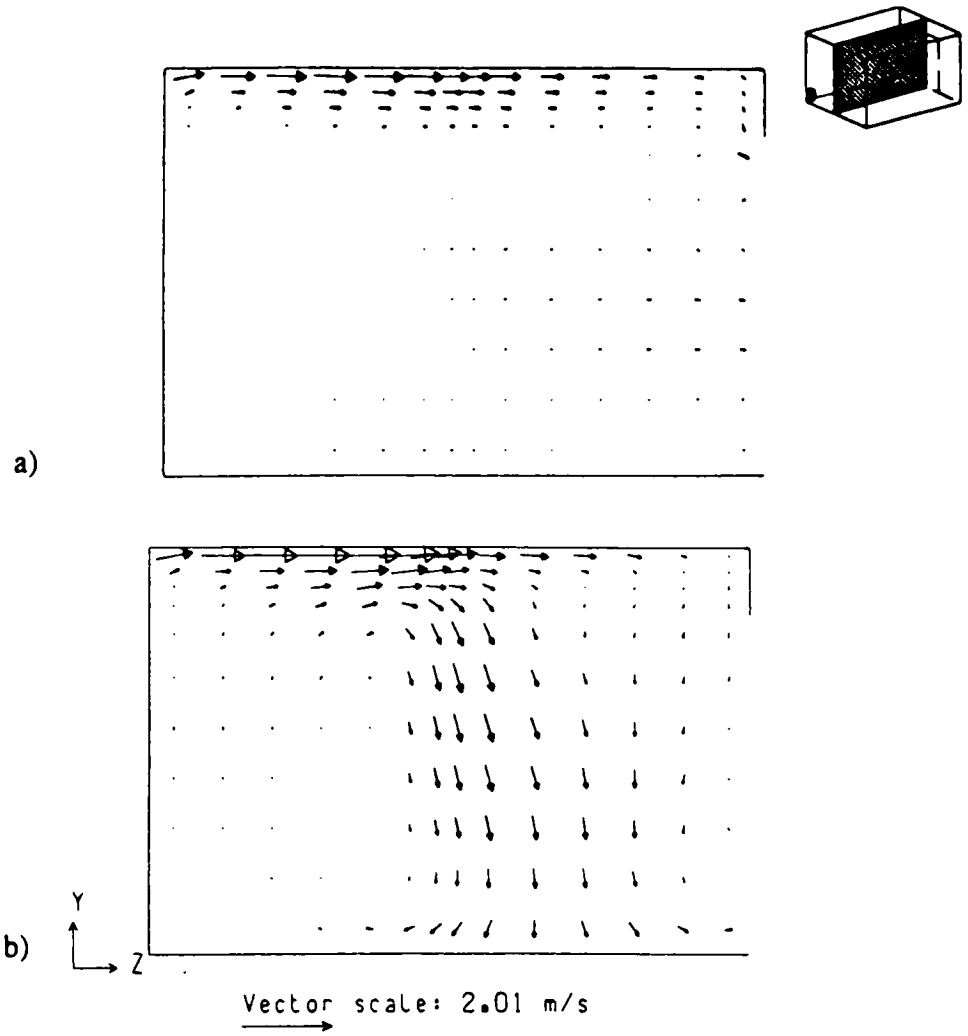

FIG. 7. Side view of office: predicted gas velocity vectors on the vertical plane through the sprinkler and doorway. (a) Fire only (175 s). (b) Fire and sprinkler (200 s).

in the spray region. In this way the life hazardous 50°C contour is in time confined to a higher level above the floor. In addition, the downward motion of the spray creates a type of water curtain which attempts to confine the hot gases to the fire end of the room.

This is more clearly observed from the gas phase velocity vectors depicted in Figure 7. Note how initially the hot gases are flowing below the ceiling and escape through the upper portions of the doorway. Meanwhile, cooler gases are entrained at the lower levels, see Fig. 7(a). However, the sprinkler churns up this stable process by mixing the hot gases with the cold water particles as they are forced out and downwards by the sprinkler. Hence, after 25 s a clear division between the two halves of the room is created. Furthermore, the gases are deflected off the floor and re-circulated within the fire side of the room.

The division of the fire compartment into hot and cold sectors is further highlighted in Fig. 8, where a horizontal plane at sprinkler height is depicted. Initially the hot fire gases were pushed into the central areas of the room and subsequently deflected and re-circulated by the confining walls in a manner similar to that observed by Satoh [13]. However, the sprinkler positioned in the centre of the compartment, presents itself as a further barrier. The hot fire gases emanating from the fire corner meet the sprinkler from where they are cooled down. Hence, cooler gases are eventually fed back into the hot upper layer, further aiding the cooling process.

This is illustrated more clearly in Fig. 9, where the associated gas velocity vectors are depicted. Here it can be seen how the circulation patterns near the doorway and west wall have changed in time.

The propagation of the water particles is illustrated in Fig. 10. The contours shown are the volume fractions of the water phase after 25 s. Note how the spray is spreading outwards asymmetrically. This could be attributed to the evaporation of the water particles as well as the direction of the main gas flow. However, due to the coarseness of the grid and the angle of

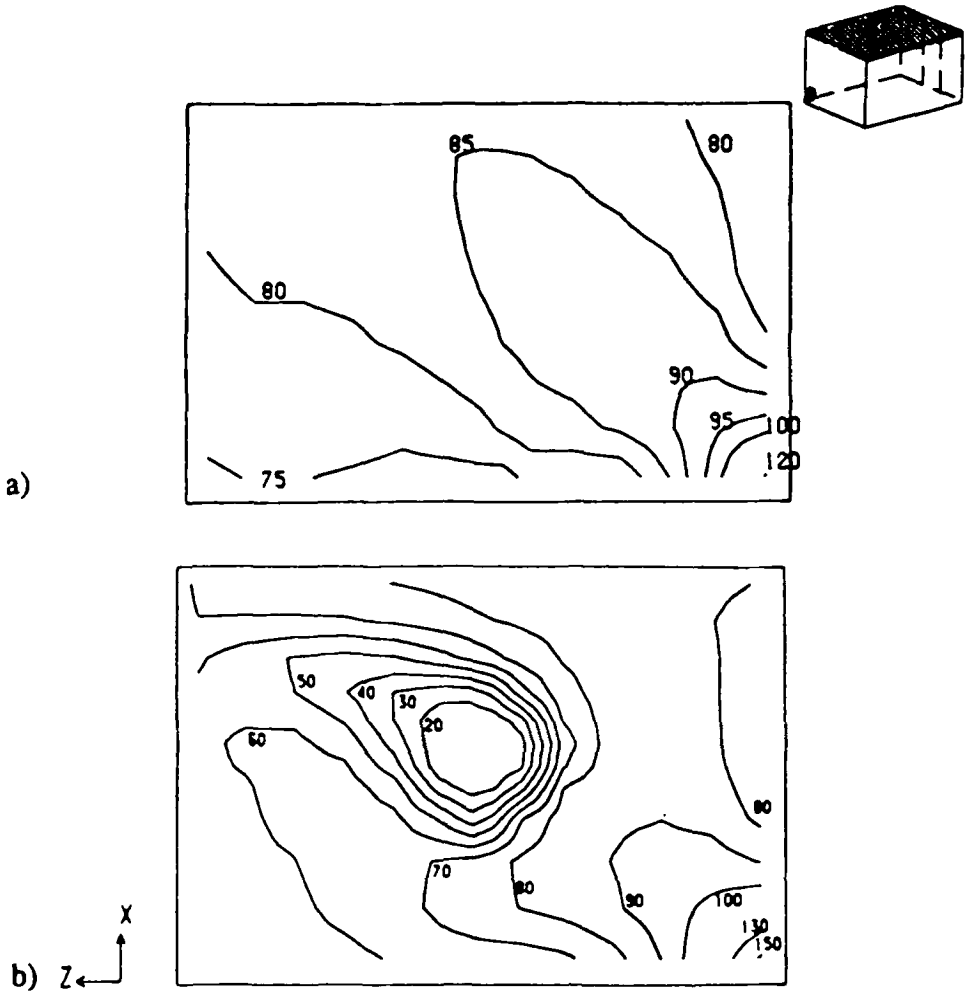

FIG. 8. Plan view of office: predicted gas temperature contours through a horizontal plane, 0.145 m below the ceiling. (a) Fire only (175 s). (b) Fire and sprinkler (200 s).

liquid injection these results are expected to suffer from false diffusion.

3.2. *Hospital ward scenario*

During the hospital ward experiment, gas temperatures were monitored at a number of locations 75 mm below the ceiling. In order to keep this description brief, results from only two positions are shown in Fig. 11. These represent the locations where the best and the least successful comparisons were made.

The first location, shown in Fig. 11(a), was situated directly above the fire source and next to the sprinkler head. It is here where the best results were obtained. The accuracy in the predictions deteriorated further away from this location, whereby Fig. 11(b) shows the poorest agreement which was located in the vicinity of the west end high corner. However, both figures once again indicate that the correct trends in temperature variations were captured.

The following figures depict gas temperatures and velocity vectors before and 120 s after sprinkler activation. Though it was not possible to compare these predictions with experimental data, they illustrate the effect the sprinkler has on the general conditions within the compartment.

The first slices shown in Figs. 12 and 13 are across the room with the heaters on the left and the elevated fire source in the centre. Though this plane is not through the actual sprinkler location, the spreading effect of the spray can clearly be identified.

Prior to sprinkler activation the fire plume was able to rise straight upwards and spread outwards along the ceiling. However, the closeness of the sprinkler once again created a form of barrier which hindered the plume from rising and spreading out. Hence, the hot temperatures are confined to below the sprinkler as well as cooling the surrounding gas temperatures. After 2 min, the gas temperatures to the right of the bed have cooled down to below 50°C. However, due to the direction of the air flow the area to the left of the bed has been kept much hotter. The velocity vectors associated with these gas temperatures are shown in

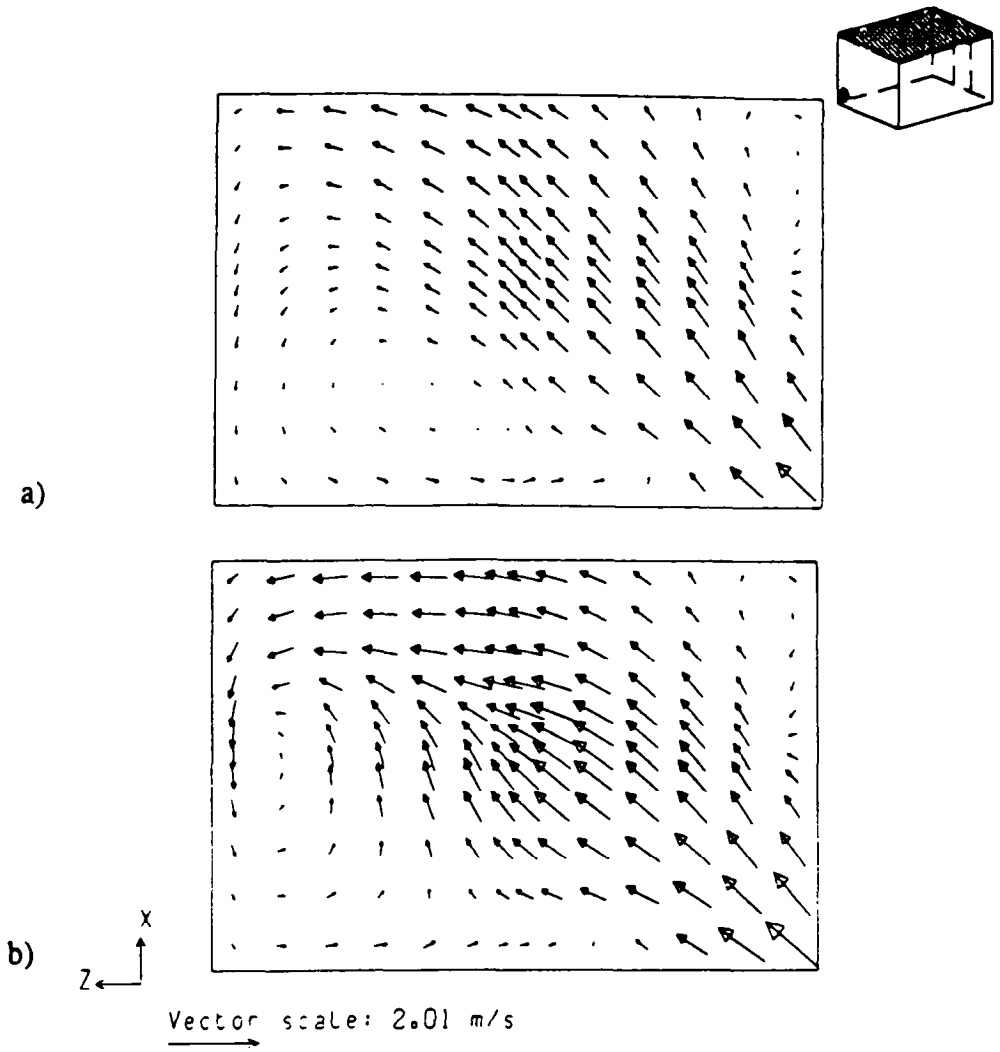

FIG. 9. Plan view of office: predicted gas velocity vectors through a horizontal plane, 0.145 m below the ceiling. (a) Fire only (175 s). (b) Fire and sprinkler (200 s).

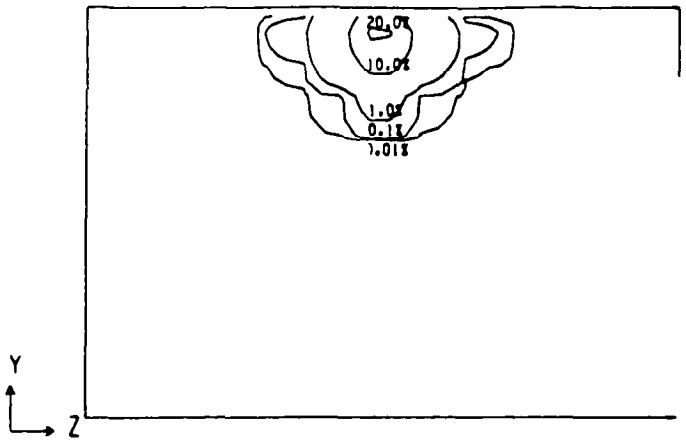

FIG. 10. Water volume fractions on the vertical central plane after 25 s of sprinkler activation.

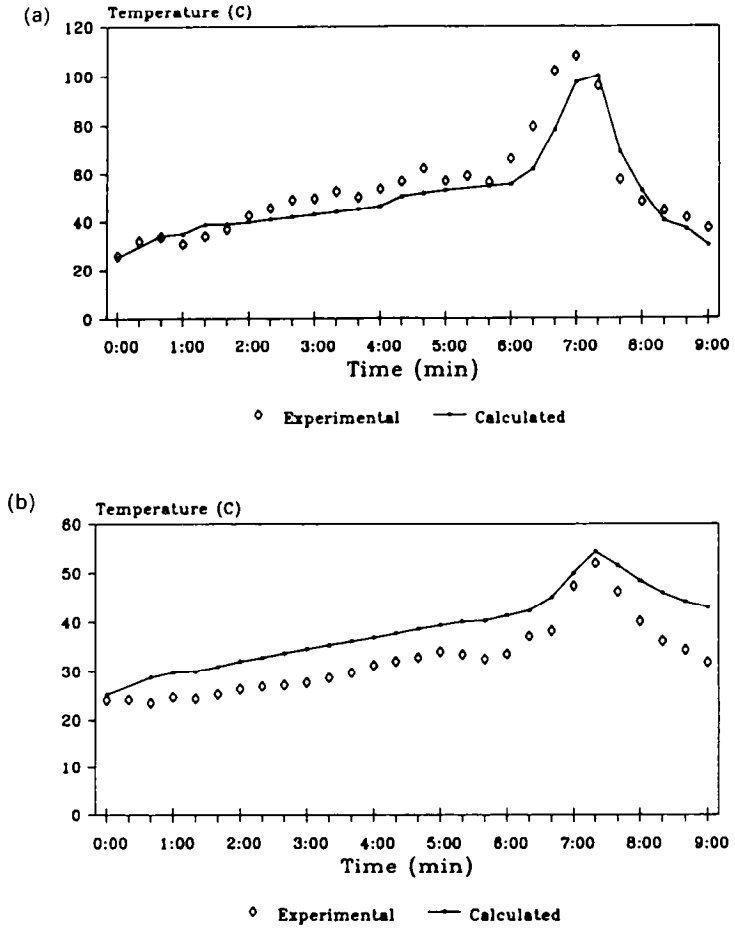

FIG. 11. Predicted and measured gas temperatures at two thermocouple locations, 0.075 m below the ceiling. (a) Located between heat source and east wall. (b) Located in the vicinity of west end high corner.

Fig. 13. Note how the entrainment is now predominantly from the right-hand side, resulting in a strong current just below the bed.

Figures 14 and 15 show gas temperatures and velocity vectors along the centre of the room through the fire and sprinkler sources.

These indicate the manner in which the sprinkler creates a water curtain confining the hot gases to a small area of the room. Eventually the gases remote from the fire and sprinkler are cooled down. Note how the hotter air layers are in fact pushed upwards due to the downwards force created by the sprinkler. In that way the life threatening 50°C level has now clearly been removed from the bulk of the compartment and confined to near the fire source, see Fig. 14(b). This effect is more clearly seen in Fig. 15 along with the overall change in flow pattern. Originally there existed one large re-circulation driven by the heat source. Two minutes after sprinkler activation two major flows are apparent. The first, generated by the sprinkler is downwards, deflecting off the bed and along the floor. The second, generated by the fire, is along the ceiling. These two currents meet towards the centre of the room, aiding the mixing and cooling process.

Finally, the spread of the water droplets in terms of their volume fractions are shown in Fig. 16 after 120 s. As in the previous case the results are expected to be influenced by false diffusion.

3.3. *Computing requirements*

A further observation to emerge from these simulations is that this approach is extremely expensive in terms of computer time. The simulations were performed on a Norsk Data ND-5900 mini-computer, roughly the equivalent to a VAX 11/780. The hospital ward calculations (see Table 1) required 75 h of CPU time to simulate the 420 s prior to sprinkler activation. The next 120 s consumed 216 h. In addition, these calculations were performed on relatively coarse grids. Clearly if this technique is to be adopted for wide scale engineering use, a means must be found of inexpensively reducing this enormous computing effort.

Parallel computing techniques offer a way of achieving this goal. At the Centre for Numerical Modelling and Process Analysis at Thames Polytechnic, a modi-

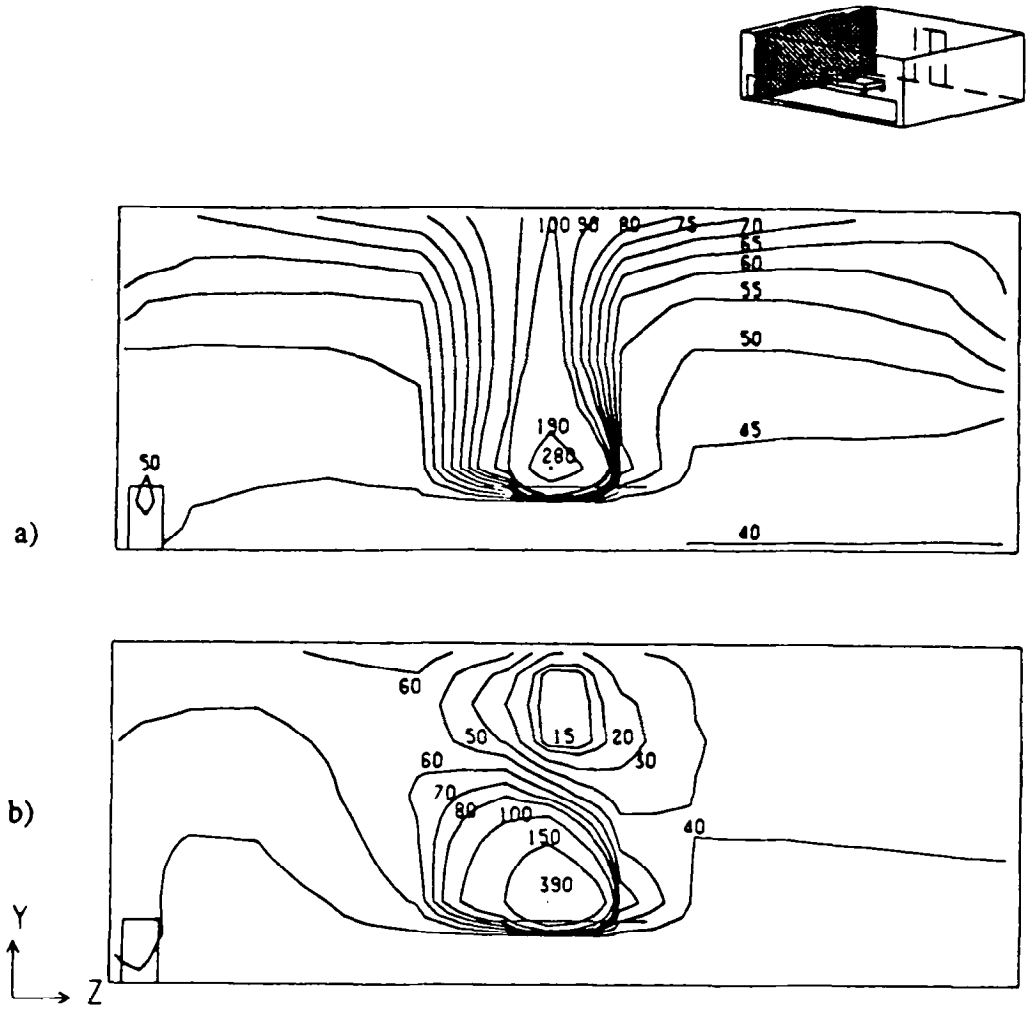

FIG. 12. Side view of hospital ward: predicted gas temperature contours along the west wall through the fire source and heaters. (a) Fire only (420 s). (b) Fire and sprinkler (540 s).

fied version of the commercial fluid flow package HARWELL-FLOW3D [14] has been produced which makes efficient use of the multi-processor architecture offered by the INMOS Transputer (Inmos, Bristol, U.K.). The original code and all modifications are implemented in FORTRAN.

The transputer is a single chip VLSI microprocessor that has been specifically designed for concurrent processing. Each T800-20 transputer is a 20 MHz 32-bit RISC microprocessor with, 4 kbytes of on-chip RAM and with many Mbytes of attached memory. It has four communication links allowing each transputer to be connected with up to four other transputers. The raw power of a T800-20 is 9 MIPS and 1.5 MFLOPS. Linpack tests using parallel FORTRAN authored by 3L Ltd (3L Ltd, Livingston, Scotland) indicate a real-

Table 1. The variation in CPU time used for the single- and two-phase simulations

Case	No. of cells	No. of phases	Simulated time (s)	CPU time (s)†	Total CPU time
Office	2640	1	175	12.5	1 day 6 h 23 min
		2	25	34.5	3 days 2 min
Hospital room	2310	1	420	13.0	3 days 3 h 13 min
		2	120	43.0	8 days 23 h 34 min

† CPU time per step per sweep.

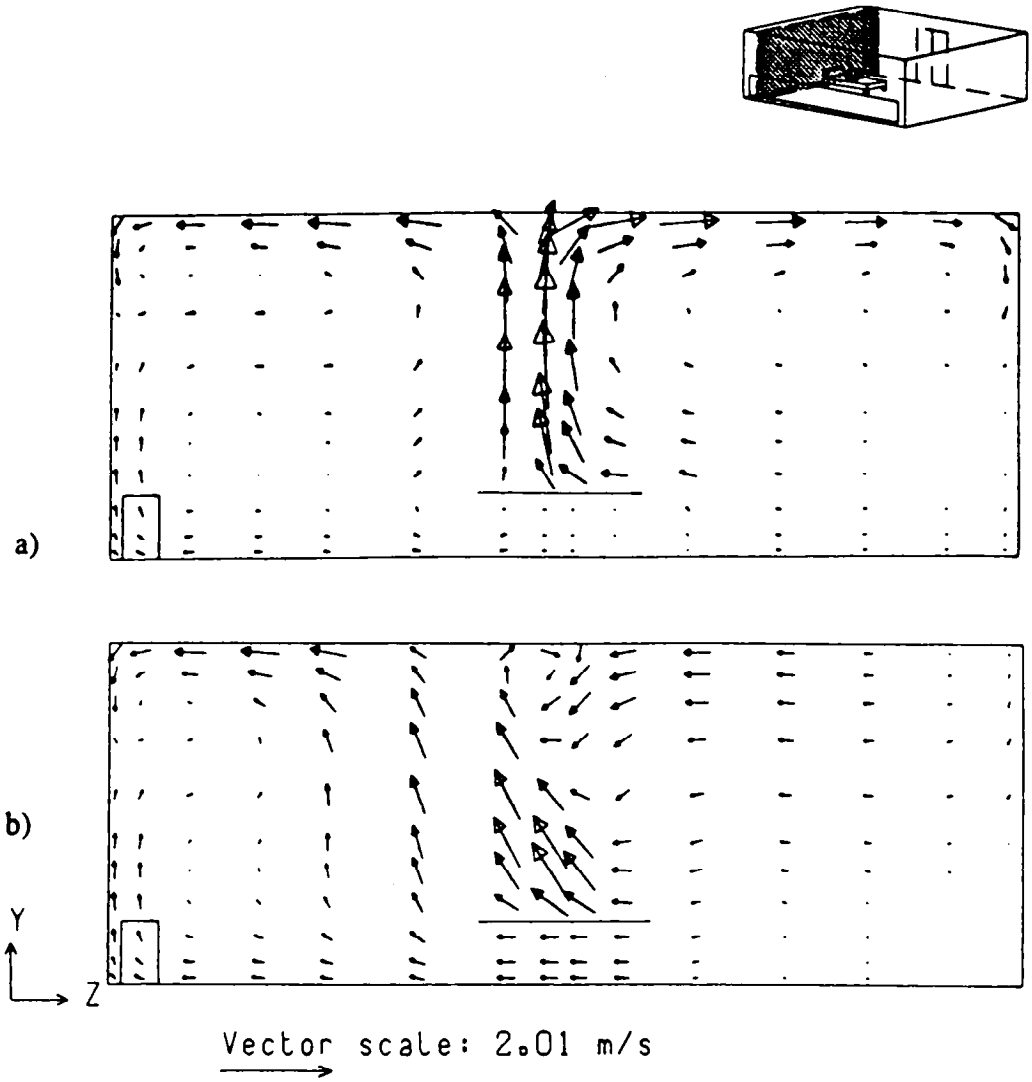

FIG. 13. Side view of hospital ward: predicted gas velocity vectors along the west wall through the fire source and heaters. (a) Fire only (420 s). (b) Fire and sprinkler (540 s).

izable performance of 0.4 MFLOPS. Fifteen transputers with over 56 Mbytes of attached memory can comfortably be hosted within a 386 AT tower case. In 1993 the T800 transputer is expected to be replaced by the T9000. This microprocessor is expected to be some 20 times faster.

General CFD test problems run using the converted HARWELL-FLOW3D code, involving up to 17 640 computational cells and utilizing 15 transputers, have revealed that efficiencies of over 86% can be achieved. On the 15 processor system this results in a 13 fold speed-up [15]. Translating this performance to the above fire–sprinkler simulation and using 30 transputers it is expected that the 291 h simulation could be performed in about 11 h. Early work utilizing this approach for fire–field model simulations indicate that this is indeed achievable [16]. In performing a 60 s single-phase fire simulation involving 24 000 cells, run times were reduced from over 4 days on a single processor to 8 h by using 15 processors.

4. CONCLUSIONS

The above two distinct fire simulations clearly indicate the complexity of fire–sprinkler interaction mechanisms. While it is still early days, the work discussed demonstrates that time-dependent fire–sprinkler simulations using the Eulerian–Eulerian approach are feasible and capable of producing qualitatively correct results. Further studies are required to investigate the effect of flow rates, droplet size, the interaction of water sprays with smoke layers and to produce grid refinement studies.

As the computational effort required to solve such problems is prohibitively expensive, it is envisaged

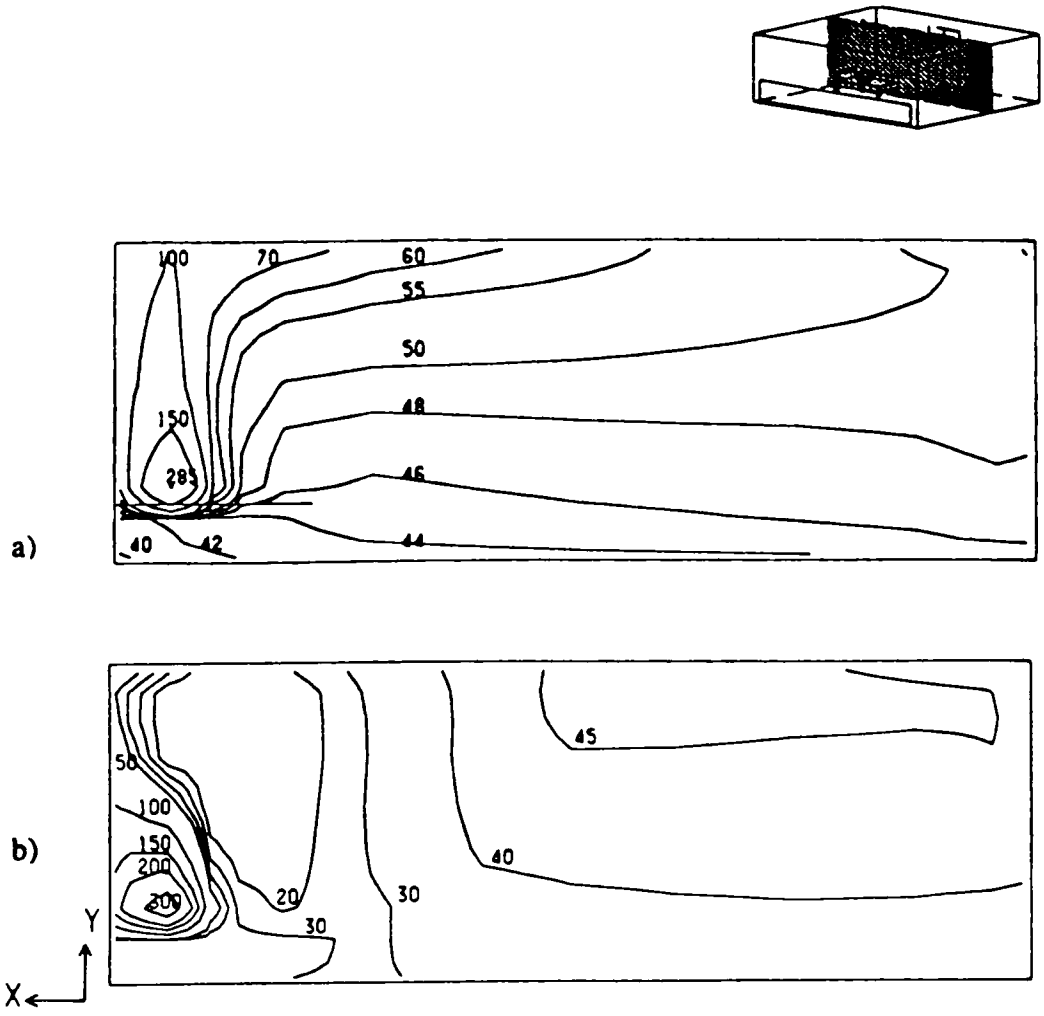

FIG. 14. Cross view of hospital ward: predicted gas temperature contours through the centre of the room, fire and sprinkler sources. (a) Fire only (420 s). (b) Fire and sprinkler (540 s).

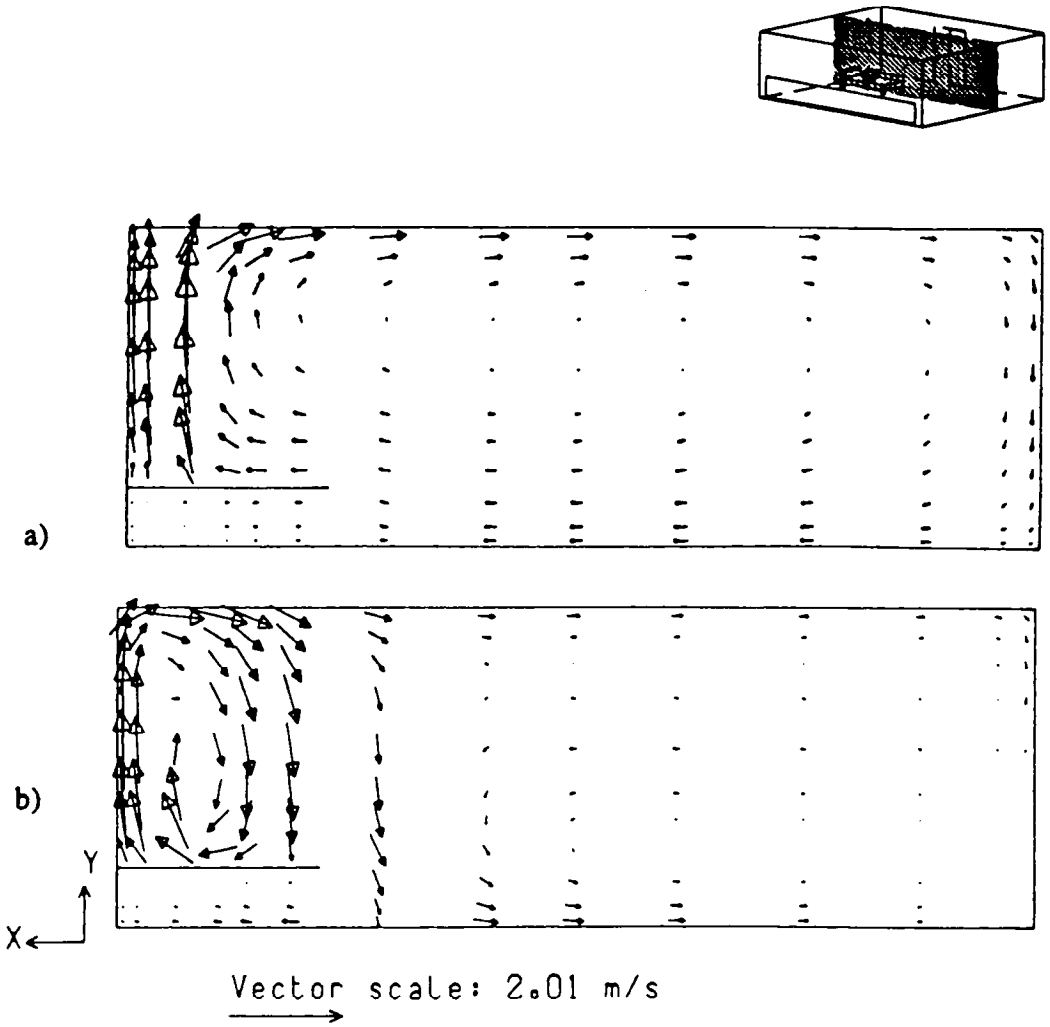

FIG. 15. Cross view of hospital ward: predicted gas velocity vectors through the centre of the room; fire and sprinkler source. (a) Fire only (420 s). (b) Fire and sprinkler (540 s).

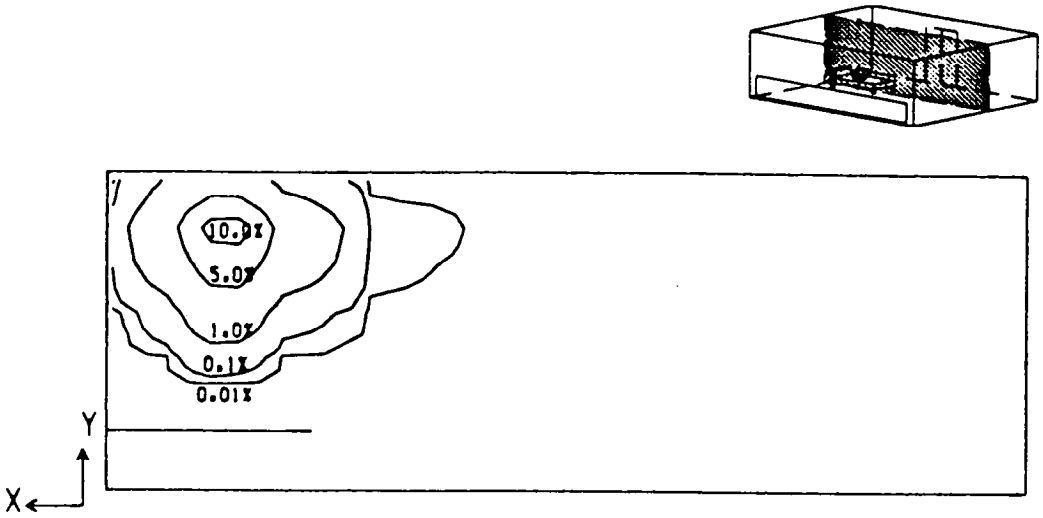

FIG. 16. Cross view of hospital ward: predicted volume fractions of water phase through the sprinkler plane.

that these studies will be performed with highly parallel architecture computers.

Furthermore, this study serves to highlight the urgent need for detailed experimental data on fire–sprinkler interaction.

Acknowledgements—The authors would like to thank Professor N. Markatos for his involvement in the early phases of this project, CHAM for allowing the use of PHOENICS, as well as the SERC and Arups for funding.

REFERENCES

1. N. A. Hoffmann and E. R. Galea, An extension of the fire–field modelling technique to include fire–sprinkler interaction—I. The mathematical basis. *Int. J. Heat Mass Transfer* **36,** 1435–1444 (1993).
2. E. R. Galea, On the field modelling approach to the simulation of enclosure fires, *J. Fire Prot. Engng* **1**(1), 11–22 (1989).
3. D. B. Spalding, A general-purpose computer program for multi-dimensional one two-phase flow, Prepr. 81–6, *Mathematics and Computers in Simulation*, Vol. 23, pp. 267–276. North-Holland (IMACS) (1981).
4. N. A. Hoffmann, Computer simulation of fire–sprinkler interaction, Ph.D. Thesis, Thames Polytechnic, London (1990).
5. N. A. Hoffman, E. Galea and N. C. Markatos, Mathematical modelling of fire sprinkler systems, *Appl. Math. Modelling* **13,** 298–306 (1989).
6. N. A. Hoffmann and E. R. Galea, The mathematical modelling of two-phase fire–sprinkler interaction, *5th European Conf. on Mathematics in Industry*, Finland, pp. 249–253. B. G. Teubner, Stuttgart and Kluwer (1990).
7. N. A. Hoffmann and E. Galea, An application of the Eulerian–Eulerian technique to a transient two-phase fire–sprinkler simulation, 13th IMACS World Congress, Dublin, Ireland (1991).
8. L. Y. Cooper and D. W. Stroup, Test results and predictions for the response of the near ceiling sprinkler links in a full-scale compartment fire, *NBSIR* 87–3633 (1987).
9. P. G. Smith, Private communication, Fire Research Station, U.K. (1987).
10. E. Galea and N. C. Markatos, The modelling and computer simulation of fire development in aircraft, *Int. J. Heat Mass Transfer* **34,** 181–197 (1991).
11. G. Heskestad and R. G. Bill, Modeling of thermal responsiveness of automatic sprinklers, *Proc. 2nd Int. Symp. on Fire Safety Science*, Tokyo, Japan, pp. 603–612 (1988).
12. H. E. Mitler, The physical basis for the Harvard computer code, Home Fire Protection Tech. Report No. 34, Harvard University (1978).
13. K. Satoh, A numerical study of ceiling jets based on 'T' pattern flames, *Proc. Fire Safety Science*, Japan, pp. 159–168. Hemisphere, Washington DC (1988).
14. A. D. Burns, I. P. Jones, J. R. Kightley and N. S. Wilkes, HARWELL-FLOW3D, User Manual (1989).
15. S. P. Johnson and M. Cross, Mapping structured grid three-dimensional CFD codes onto parallel architectures, *Appl. Math. Modelling* **15,** 394–405 (1991).
16. C. S. Ierotheou and E. R. Galea, A fire field model implemented in a parallel computing environment, *Int. J. Numer. Meth. Fluids* **14,** 175–187 (1992).